Journal of Alloys and Compounds 506 (2010) 253–262

Contents lists available at ScienceDirect

Journal of Alloys and Compounds

journal homepage: www.elsevier.com/locate/jallcom

Phase transformation of metastable cubic γ-phase in U–Mo alloys

V.P. Sinha[a,*], P.V. Hegde[a], G.J. Prasad[a], G.K. Dey[b], H.S. Kamath[a]

[a] Metallic Fuels Division, Bhabha Atomic Research Centre, Mumbai 400085, India
[b] Material Science Division, Bhabha Atomic Research Centre, Mumbai 400085, India

ARTICLE INFO

Article history:
Received 4 May 2010
Accepted 30 June 2010
Available online 7 July 2010

Keywords:
Phase
Metastable
Density
X-ray diffraction
Alloy and microstructure

ABSTRACT

Over the past decade considerable efforts have been put by many fuel designers to develop low enriched uranium (LEU < 20%U^{235}) base U–Mo alloy as a potential fuel for core conversion of existing research and test reactors which are running on high enriched uranium (HEU > 85%U^{235}) fuel and also for the upcoming new reactors. U–Mo alloy with minimum 8 wt% molybdenum shows excellent metastability with cubic γ-phase in cast condition. However, it is important to characterize the decomposition behaviour of metastable cubic γ-uranium in its equilibrium products for in reactor fuel performance point of view. The present paper describes the phase transformation behaviour of cubic γ-uranium phase in U–Mo alloys with three different molybdenum compositions (i.e. 8 wt%, 9 wt% and 10 wt%). U–Mo alloys were prepared in an induction melting furnace and characterized by X-ray diffraction (XRD) method for phase determination. Microstructures were developed for samples in as cast condition. The alloys were hot rolled in cubic γ-phase to break the cast structure and then they were aged at 500 °C for 68 h and 240 h, so that metastable cubic γ-uranium will undergo eutectoid decomposition to form equilibrium phases of orthorhombic α-uranium and body centered tetragonal U_2Mo intermetallic compound. U–Mo alloy samples with different ageing history were then characterized by XRD for phase and development of microstructure.

1. Introduction

Due to concern on nuclear proliferation and diversion the reduced enrichment for research and test reactor (RERTR) programme was initiated in US in the late-1970s with the development of new fuels that will allow the use of low enriched uranium (LEU < 20%U^{235}) in the world's research and test reactors that were fueled by high enriched uranium (HEU > 85%U^{235}) and also in the to be built research and test reactors [1]. Developing nuclear fuel cycle based on LEU means either one has to increase the fuel loading in the meat or develop high density uranium compounds/alloys to compensate the lower enrichment. The two most common fuel fabrication processes to make LEU fuel without significant alteration in the fuel core configuration in the reactor are namely roll bonding process for plate geometry and extrusion process for rod or tube geometry [2–4]. Roll bonding process is suitable for fuel particle loading up to around 55 vol% and extrusion method is likely to have a lower maximum fuel particle volume limit than roll bonding [5,6]. Due to limitation on the increase of fuel volume fraction in the fuel meat, the only other option is to increase the heavy metal (i.e. uranium) density of the fuel itself. It has been demonstrated that aluminium base dispersion fuel with U_3Si_2 as fuel material is very successful in converting reactor cores which requires fuel element loading of up to about 5 g U cm^{-3} [7,8]. However, still higher uranium density fuel compounds/alloys are required to be developed to fulfill the objective of developing a fuel system which can achieve a heavy metal density of 8–9 g U cm^{-3}, as many of the researchers wanted to develop a neutron source with high thermal neutron flux density for superior quality experiments [9]. The use of higher uranium density compounds like U_3Si and U_6Me where Me can be Fe, Ni, Mn, Co or Ge were proved unsuccessful for dispersion fuel application because they exhibit high swelling rate (break away swelling) even at relatively low burnups [10–12].

Uranium metal density of the order of 8–9 g U cm^{-3} in the fuel meat can be achieved with the use of pure uranium metal or uranium alloys as dispersoids. The room temperature phase of pure uranium (i.e. α-uranium having orthorhombic crystal structure) shows very poor irradiation stability (even under low burnups and high temperature irradiation conditions) due to cavitational swelling under irradiation and thermal growth under power ramping which makes it unsuitable as fuel [13–15]. On the other hand the high temperature phase of pure uranium (i.e. γ-uranium having body centered cubic crystal structure) is quite stable under irradiation than α-uranium since swelling takes place here mainly due to fission gas nucleation and growth mechanism. Thermodynamically high temperature pure cubic γ-uranium is not stable under preparation and irradiation condition. However, there are some alloying

* Corresponding author at: Metallic Fuels Division, Bhabha Atomic Research Centre, Trombay, Mumbai 400085, India. Tel.: +91 22 25590697; fax: +91 22 25505151.
E-mail address: vedsinha@barc.gov.in (V.P. Sinha).

0925-8388/$ – see front matter © 2010 Elsevier B.V. All rights reserved.
doi:10.1016/j.jallcom.2010.06.187

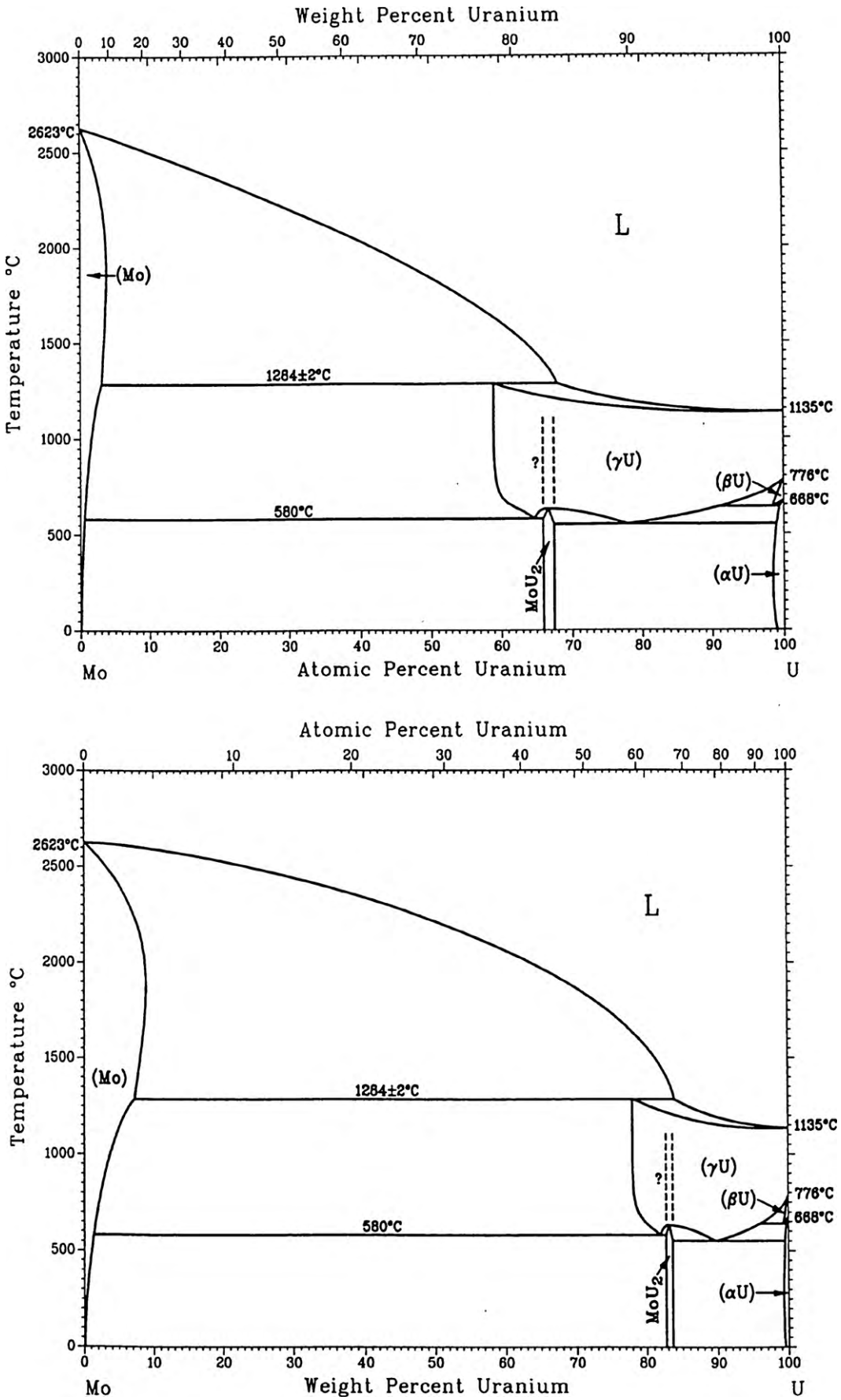

Fig. 1. Uranium–molybdenum phase diagram.

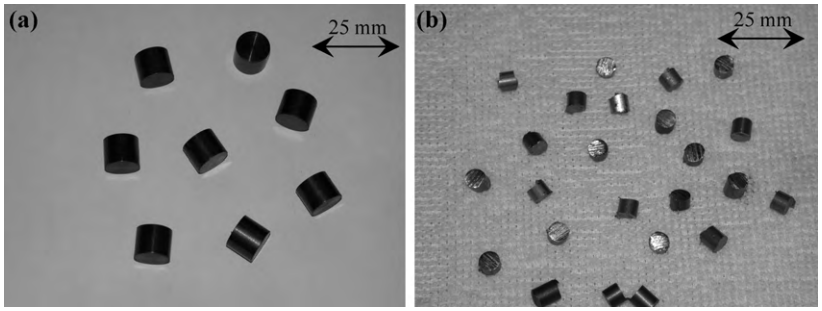

Fig. 2. Photograph of (a) uranium metal pellets and (b) molybdenum metal pieces.

Table 1
Weights of starting constituent elements and cast U–Mo alloys.

Composition of U–Mo alloy	Uranium weight (g)	Molybdenum weight (g)	U–Mo alloy ingot weight (g)
U–8 wt%Mo	63.4	5.46	68.87
U–9 wt%Mo	64.79	6.41	71.24
U–10 wt%Mo	67.11	7.40	74.53

elements which can make the high temperature pure γ-uranium metastable at room temperature. Several transition metals, particularly from Group IVA to Group VIIIA of periodic table form solid solution with γ-U, which can be retained as metastable phase at room temperature upon cooling. The stabilizing power of these elements increases with their atomic number since more and more *d*-electrons will participate in bonding due to hybridization with s and p orbital electrons. However, their solubility will decrease as the size difference with uranium atom increases. In fact the increase in bond strength with the increase in atomic number of transition elements will promote the formation of intermetallic compound rather than a solid solution. The uranium alloys which have a tendency to form stable cubic phase at room temperature are U–Zr, U–Mo, U–Nb, U–Re, U–Ru, U–Ti, etc. [16]. The first two transition elements of 4d series (i.e. Zr and Nb) will form complete solid solution with γ-uranium. But to retain the 100% γ-phase at room temperature, large concentration of these elements are required to be added in the alloy. On the other extreme Pd and Pt have only ~2 at% solubility in γ-uranium and these alloying elements will give very stable intermetallic compounds with uranium. It was earlier recognized that molybdenum is a good compromise for the two extremes mentioned above [17].

In uranium molybdenum system below 560 °C the γ-phase can exist only in a metastable state because under equilibrium cooling below 560 °C, the cubic γ-phase with the space group *Im*3*m* will break into orthorhombic α-phase of space group *Cmcm* and body centered tetragonal γ′-phase (U_2Mo) of space group *I*4/*mmm* (see Fig. 1). Therefore, the prospect of using a U–Mo alloy as reactor fuel is closely connected with the possibility of retaining a metastable γ-phase in alloys at temperature below 560 °C during fuel fabrication and irradiation. The metastable cubic γ-phase can be retained below 560 °C either by rapid cooling from γ-phase field or by adding sufficient quantities of molybdenum as alloying element in uranium under normal furnace cooling condition. It has been reported that U-alloys with maximum 11 at% Mo when water quenched from γ-phase field will transform into metastable α′ and α″ phases, which are slight variant of the orthorhombic lattice of α-U. Alloys containing 11.39–12.73 at% Mo, when water quenched will form an ordered γ°-phase with an ordered tetragonal structure [18–22]. Hence water quenched uranium alloys containing up to about 11 at% Mo are termed as "alpha phase" alloys and with more than 11 at% Mo as "gamma phase" alloys.

In connection with dispersion fuel development work at BARC, R & D efforts are on to develop high density uranium alloys/compounds to fulfill certain departmental objective [17,23,24] and also address the international concern on proliferation. Under this programme U–Mo alloys with three different molybdenum compositions (i.e. U–8 wt%Mo, U–9 wt%Mo and U–10 wt%Mo) have been prepared by induction melting route. The as cast alloy samples were then hot rolled in the γ region of U–Mo phase diagram to break the cast structure and were cooled to room temperature. These alloy samples were heat treated at 500 °C for

Fig. 3. Photograph of as cast U–Mo alloy ingots.

Fig. 4. Photograph of copper jacketed as cast U–Mo alloy samples.

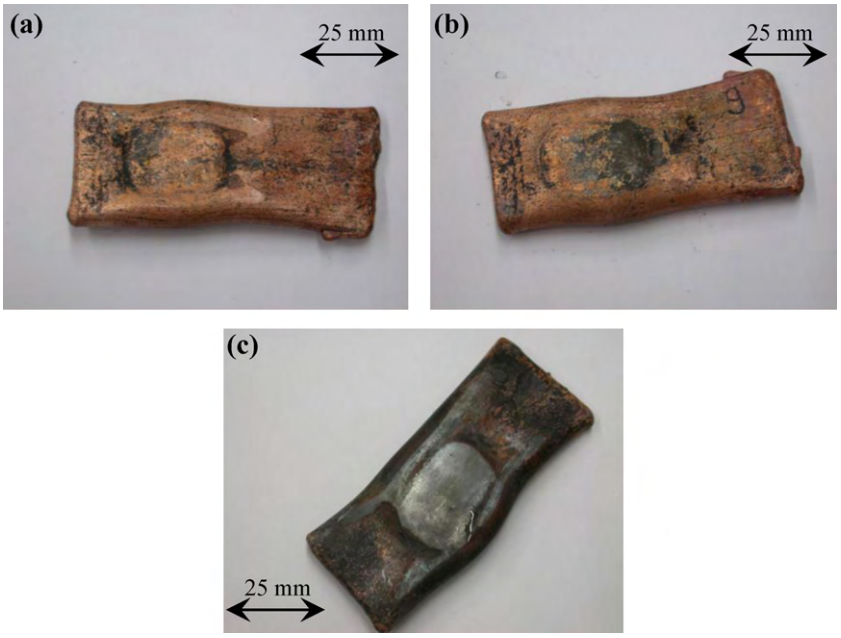

Fig. 5. Photograph of rolled copper jacketed U–Mo alloy samples (a) U–8 wt%Mo, (b) U–9 wt%Mo and (c) U–10 wt%Mo.

Table 2
Description of etchants used for U–Mo alloys after rolling and ageing.

Composition of alloy	Etchant composition and process details
Rolled U–8 wt%Mo, U–9 wt%Mo and U–10 wt%Mo	1 part orthophosphoric acid, 2 part H_2SO_4 and 2 part H_2O. Used as chemical etchant, freshly polished sample is attacked with few drops.
Aged U–8 wt%Mo, U–9 wt%Mo and U–10 wt%Mo	5 part orthophosphoric acid and 100 part H_2O. 2–2.5 V open circuit, stainless steel cathode is used for electrolytic etching.

different durations so that γ-phase of uranium will undergo eutectoid decomposition to form equilibrium composition of α-uranium and U_2Mo intermetallic. The heat treated alloy samples were then characterized by XRD for phase analysis and microstructure was developed for each U–Mo alloy with different heat treatment history. The lattice parameter of γ-phase of U–Mo alloys with three different molybdenum compositions in as cast, hot rolled and after heat treated condition were calculated and reported in the paper. The lattice parameter of α-phase has also been calculated for heat treated U–Mo alloys and reported. The precise lattice parameter calculation was done using CELREF programme [25]. Optical microstructures of various U–Mo alloys were also evaluated by image analysis for quantifying different phases present.

2. Experimental work

2.1. Alloy preparation

U–Mo alloys were prepared in an induction furnace with cylindrical uranium metal pellets (shown in Fig. 2(a)) and molybdenum metal pieces (shown in Fig. 2(b)) as starting material. Chemical analysis of uranium metal pellets and molybdenum metal pieces shows 99.9 wt% 'U-content' and 99.8 wt% 'Mo-content', respectively. Uranium metal pellets were cleaned electrochemically using orthophosphoric acid as electrolyte in a stainless steel container with 20 V of DC supply while molybdenum metal pieces were cleaned in an ultrasonic cleaner. Uranium metal pellets with typical dimension of 12 mm diameter and around 10 mm in length were charged in yttria coated graphite crucible along with molybdenum metal pieces with around 3.5 mm diameter and 2.5 mm in length in required proportion. The crucible was loaded in an induction furnace and was flushed thrice with ultra high purity argon gas to remove any traces of oxygen. The furnace was heated up to a temperature of 1300 ± 10 °C with 30 min of soaking under vacuum of 10^{-5} mbar. The molten alloy was then furnace cooled to room temperature and ingot of U–Mo alloy was taken out by cleaning the graphite crucible in an ultrasonic cleaner. Three types of U–Mo alloys with different molybdenum percentage (i.e. U–8 wt%Mo, U–9 wt%Mo and U–10 wt%Mo) were prepared by the same method (see Fig. 3). The U–Mo alloy ingots thus prepared were of typical dimension of around 15 mm diameter and 40 mm length. The final weight of all alloy ingots was recorded and is shown in Table 1.

2.2. Hot rolling

Cast U–Mo alloy samples were then subjected to hot rolling operation to break the as cast structure for which the ingots were jacketed in copper casing (see Fig. 4). The copper jacketed alloy ingots were heated in a resistance heating furnace at 900 °C which is the γ-phase region in U–Mo phase diagram (see Fig. 1) and 100% metastable cubic γ-phase can be retained at room temperature with the minimum 8 wt% molybdenum addition in uranium as solute in as cast condition. The copper jacketed pieces were then hot rolled to reduce the ingot cross-section by more than 50% to get 50% hot working condition in the alloy samples (see Fig. 5). Then the U–Mo alloy ingots were dejacketed from copper casing and the hot worked alloy pieces were cleaned in an ultrasonic cleaner.

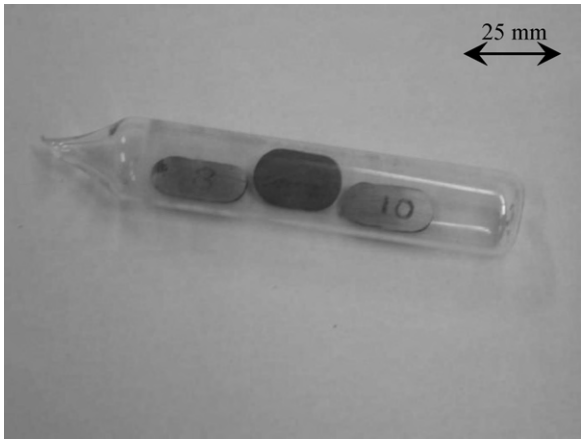

Fig. 6. Photograph of quartz encapsulated U–Mo alloy pieces.

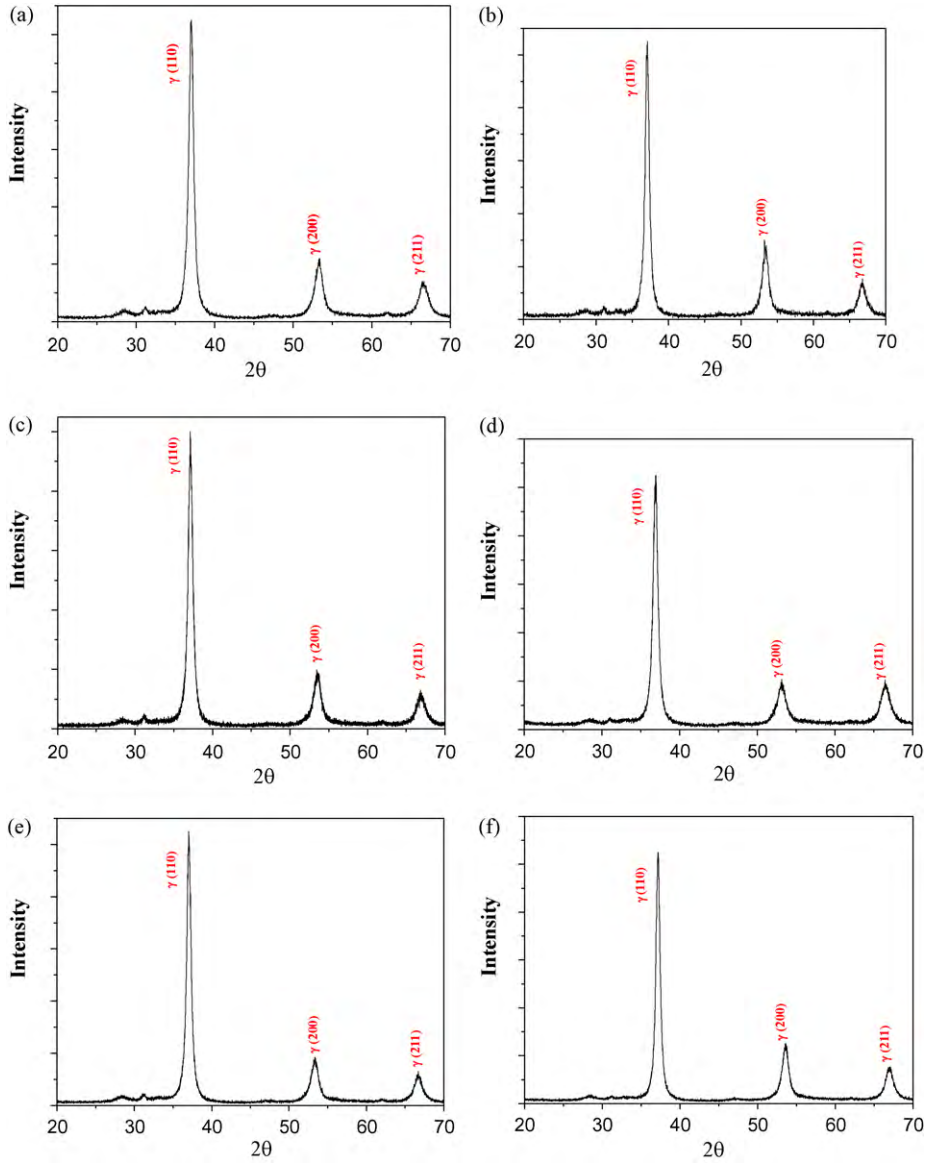

Fig. 7. X-ray diffraction pattern of as cast alloy (a) U–8 wt%Mo, (b) U–9 wt%Mo and (c) U–10 wt%Mo; hot rolled alloy (d) U–8 wt%Mo, (e) U–9 wt%Mo and (f) U–10 wt%Mo.

2.3. Ageing

After hot working the U–Mo alloy ingots were encapsulated in quartz tube under the partial pressure of helium (see Fig. 6). The U–Mo alloy ingots were then aged in a resistance heating furnace at 500 °C for 68 h and 240 h so that γ-phase will undergo eutectoid decomposition to form equilibrium α-phase and U_2Mo intermetallic. Two sets of quartz encapsulated U–Mo pieces were prepared for two different ageing treatments. The aged alloy pieces were then taken out by breaking the quartz tube at room temperature.

2.4. Characterization

After rolling and ageing treatment the cast U–Mo alloy samples were characterized by XRD for phase determination. XRD sample was prepared by cutting a disk of around 15 mm diameter and 2 mm thickness from the alloy ingots in SiC cut-off wheel. The disks were then mounted and polished by 2 μm diamond paste in standard metallographic set up to get good surface finish. The polished samples were then scanned in standard theta–theta XRD equipment with a scan rate of 0.5° per minute. Standard source of Cu Kα radiation with curved graphite monochromater

Table 3
Precise lattice parameter and lattice volume of orthorhombic α-uranium in aged U–Mo alloys.

Composition of alloy	Precise lattice parameter of α-uranium (Å)			Lattice volume (Å^3)
	a	*b*	*c*	
Unalloyed α-uranium at RT	2.8540	5.8700	4.9550	83.0110
U–8 wt%Mo after ageing for 68 h at 500 °C	2.8533	5.8595	4.9549	82.8405
U–8 wt%Mo after ageing for 240 h at 500 °C	2.8528	5.8628	4.9560	82.8911
U–9 wt%Mo after ageing for 68 h at 500 °C	2.8528	5.8607	4.9565	82.8696
U–9 wt%Mo after ageing for 240 h at 500 °C	2.8563	5.8658	4.9541	83.0034
U–10 wt%Mo after ageing for 68 h at 500 °C	2.8519	5.8638	4.9546	82.8556
U–10 wt%Mo after ageing for 240 h at 500 °C	2.8542	5.8606	4.9601	82.9692

Table 4
Precise lattice parameter and lattice volume of cubic γ-uranium in hot rolled U–Mo alloys.

Composition of alloy	Precise lattice parameter of γ-uranium (Å)	Lattice volume (Å^3)
Unalloyed γ-uranium	3.4740	41.9266
Rolled U–8 wt%Mo	3.4432	40.8213
Rolled U–9 wt%Mo	3.4308	40.3818
Rolled U–10 wt%Mo	3.4141	39.7950

and sealed proportional counter was used in the machine. Instrument was operated at 1 kW with tube voltage and tube current at 35.0 kV and 28.4 mA, respectively, to generate XRD patterns for all the U–Mo alloy samples. By using CELREF programme precise lattice parameter was calculated for each cast alloy sample after rolling and ageing treatment.

Microstructure was also developed for each alloy composition after rolling and with different ageing history. Samples were cut to size of around 15 mm diameter and 4 mm thickness by using SiC cut-off wheel. The disks were mounted and then grinding and polishing was done for each sample using standard metallographic procedures to get scratch free surface. The polished samples were then etched to develop desired microstructure. Different etchants were used for as cast, rolled and aged U–Mo alloy samples (see Table 2).

3. Results and discussion

In uranium molybdenum alloys the cubic γ-phase can be retained at room temperature with the addition of minimum 8 wt% Mo under furnace cooling condition and with 10 at% Mo under critical cooling conditions [19]. However, it is very important to examine the metastability of cubic phase at higher temperatures for better understanding of fuel behaviour and performance in reactor. It is seen from the U–Mo phase diagram (see Fig. 1) that the cubic phase is stable above 560 °C but as the temperature go below this critical temperature it will undergo eutectoid decomposition to form orthorhombic α-phase and body centered tetragonal intermetallic compound U_2Mo. The classification of U–Mo alloys in respect to their eutectoid decomposition becomes more appreciable as orthorhombic α-phase of uranium has very little solid solubility for molybdenum and this phase does not have good irradiation properties. This is very much evident from the fact that the α-phase is formed due to the eutectoid decomposition of γ-phase after ageing of U–Mo alloys which does not show any significant change in the lattice parameter (see Table 3). U–Mo alloy ingots were hot rolled before doing the ageing treatment so that no artefacts are there during microstructural evaluation. The precise lattice parameter of hot rolled U–Mo alloy samples were calculated and compared with that of cast structure samples (see Table 4) which shows complete recrystallization of γ grains during the process.

3.1. Phase analysis

The XRD pattern of U–8 wt%Mo, U–9 wt%Mo and U–10 wt%Mo alloy in as cast condition and hot rolled condition shows only the presence of cubic γ-phase (see Fig. 7). The presence of γ-phase in all the three compositions of hot rolled U–Mo alloys (i.e. U–8 wt%Mo, U–9 wt%Mo and U–10 wt%Mo) confirms the fact that rolling was performed in γ-phase field and no oxygen pick up took place during the process. XRD pattern of U–8 wt%Mo alloy (see Fig. 8(a)), U–9 wt%Mo alloy (see Fig. 8(b)) and U–10 wt%Mo alloy (see Fig. 8(c)) on ageing at 500 °C for 68 h clearly shows the presence of orthorhombic α-phase, U_2Mo intermetallic and cubic γ-phase. It is also seen from their XRD pattern that the relative peak intensity for orthorhombic α-phase and U_2Mo intermetallic is low with the increase of molybdenum content. The XRD pattern of U–8 wt%Mo alloy (see Fig. 9(a)), U–9 wt%Mo alloy (see Fig. 9(b)) and U–10 wt%Mo alloy (see Fig. 9(c)) on ageing at 500 °C for 240 h also shows the presence of orthorhombic α-phase, U_2Mo intermetallic and cubic γ-phase. The relative peak intensity of eutectoid decom-

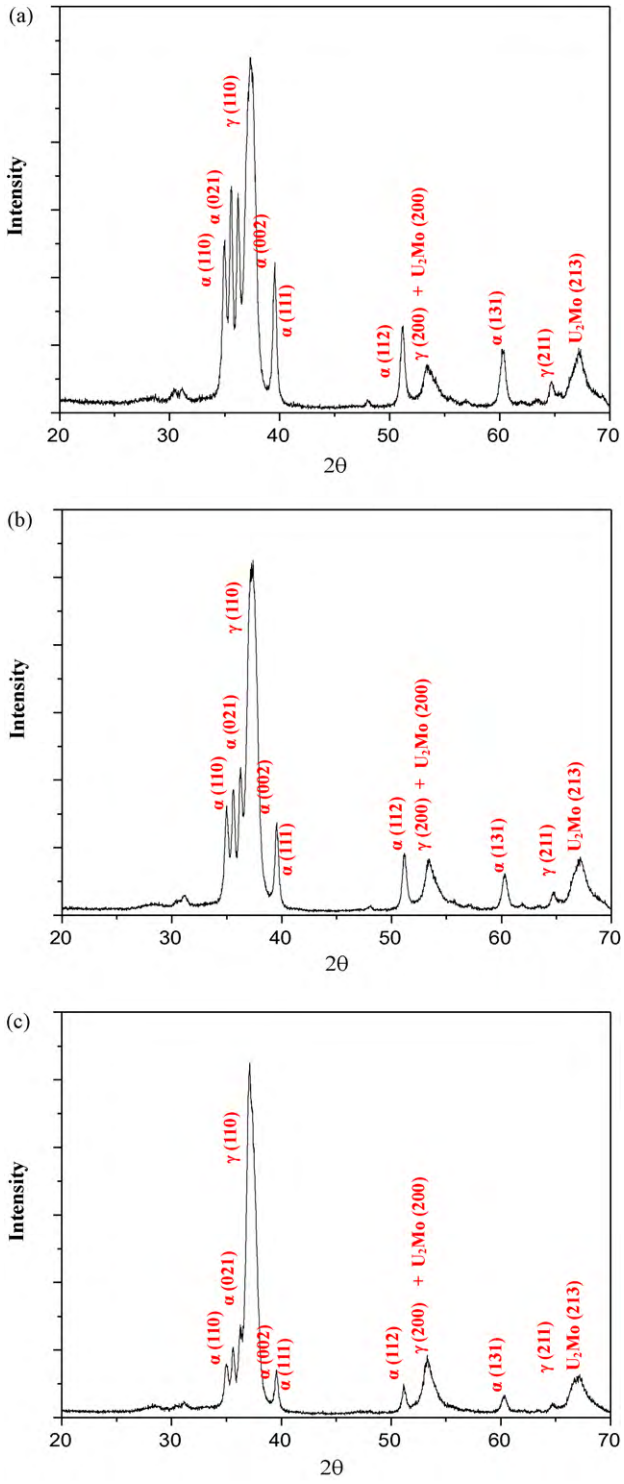

Fig. 8. X-ray diffraction pattern of aged U–Mo alloy at 500 °C for 68 h (a) U–8 wt%Mo, (b) U–9 wt%Mo and (c) U–10 wt%Mo.

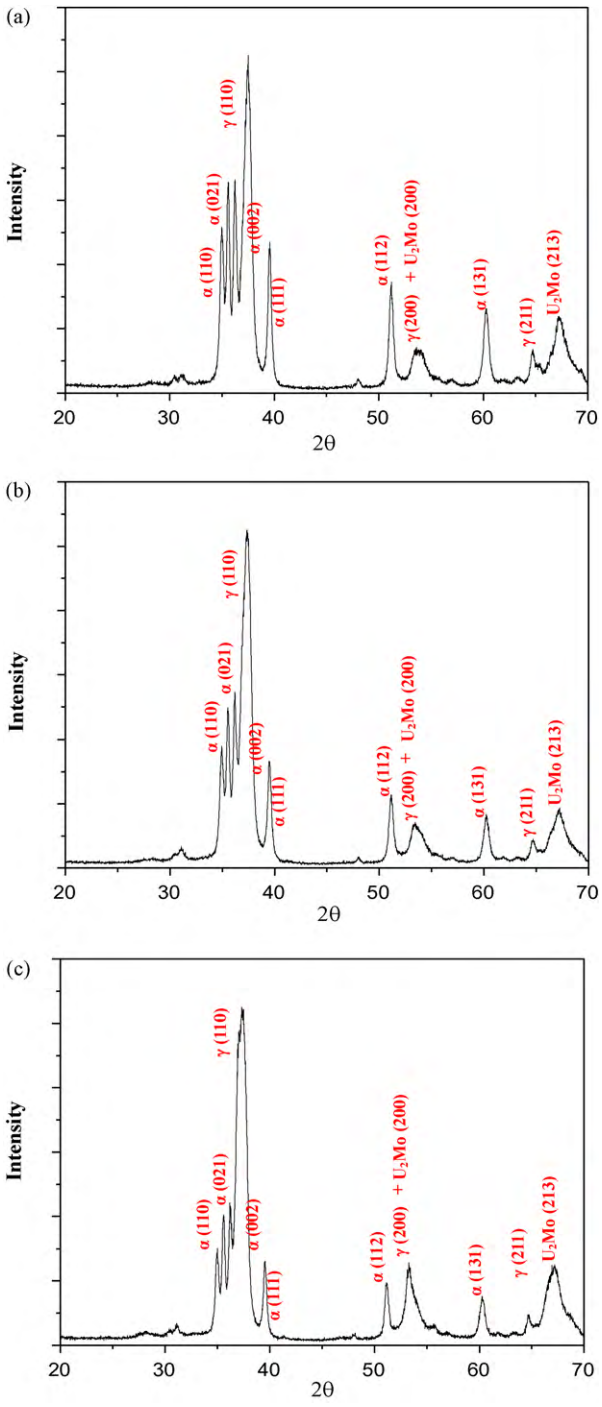

Fig. 9. X-ray diffraction pattern of aged U–Mo alloy at 500 °C for 240 h (a) U–8 wt%Mo, (b) U–9 wt%Mo and (c) U–10 wt%Mo.

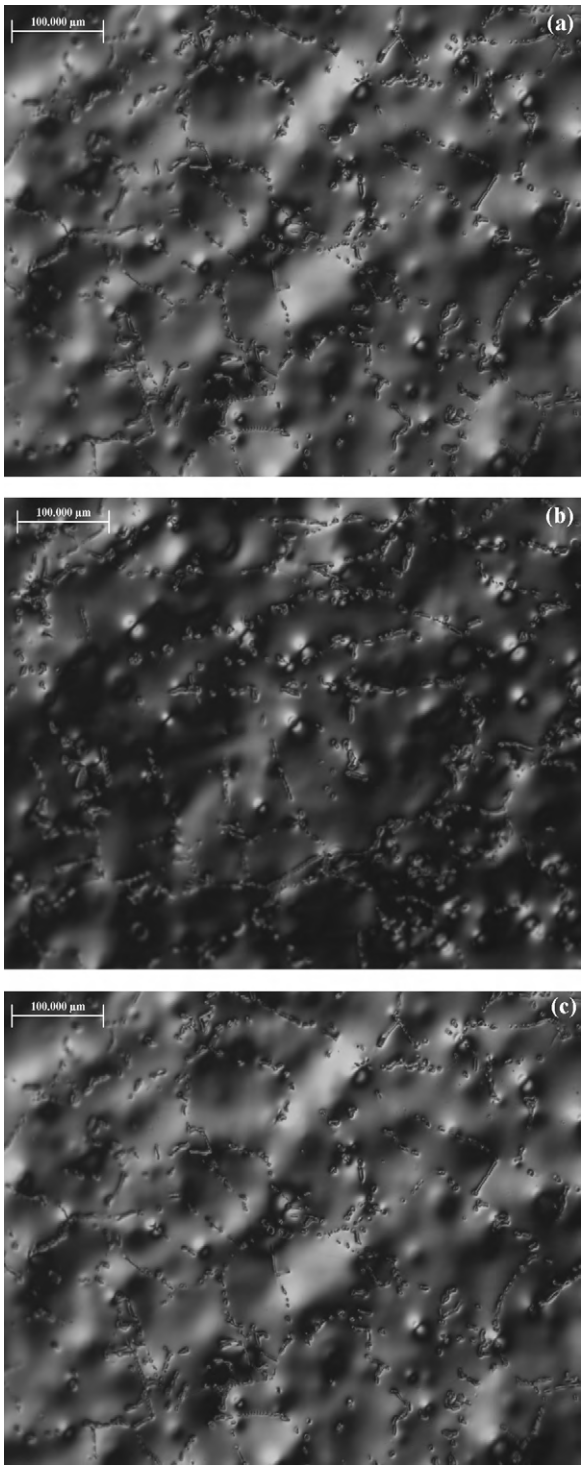

Fig. 10. Microstructure of hot rolled U–Mo alloy (a) U–8 wt%Mo, (b) U–9 wt%Mo and (c) U–10 wt%Mo.

posed product is low with the increase of molybdenum content in uranium. It is also seen that the peak sharpness of cubic γ-phase in case of U–Mo alloys aged for 240 h is more as compare to the aged U–Mo alloys for 68 h, which means that the cubic γ-phase is more homogeneous in terms of molybdenum distribution after 240 h of heat treatment as compare to 68 h of heat treatment.

3.2. Calculation of precise lattice parameter

CELREF programme was used for the calculation of precise lattice parameter of cubic γ-uranium unit cell for each U–Mo alloy. The programme uses method of least squares to determine for cell refinement [25]. The precise lattice parameter thus calculated for orthorhombic α-phase and cubic γ-phase for all the three compositions after hot rolling, and ageing treatment is shown in Table 3. It can be seen that there is not much change in the lattice parameter of orthorhombic α-phase even after ageing it for 68 h and 240 h, indicating that the solid solubility of molybdenum in α-uranium at room temperature remains same (around 1 at%).

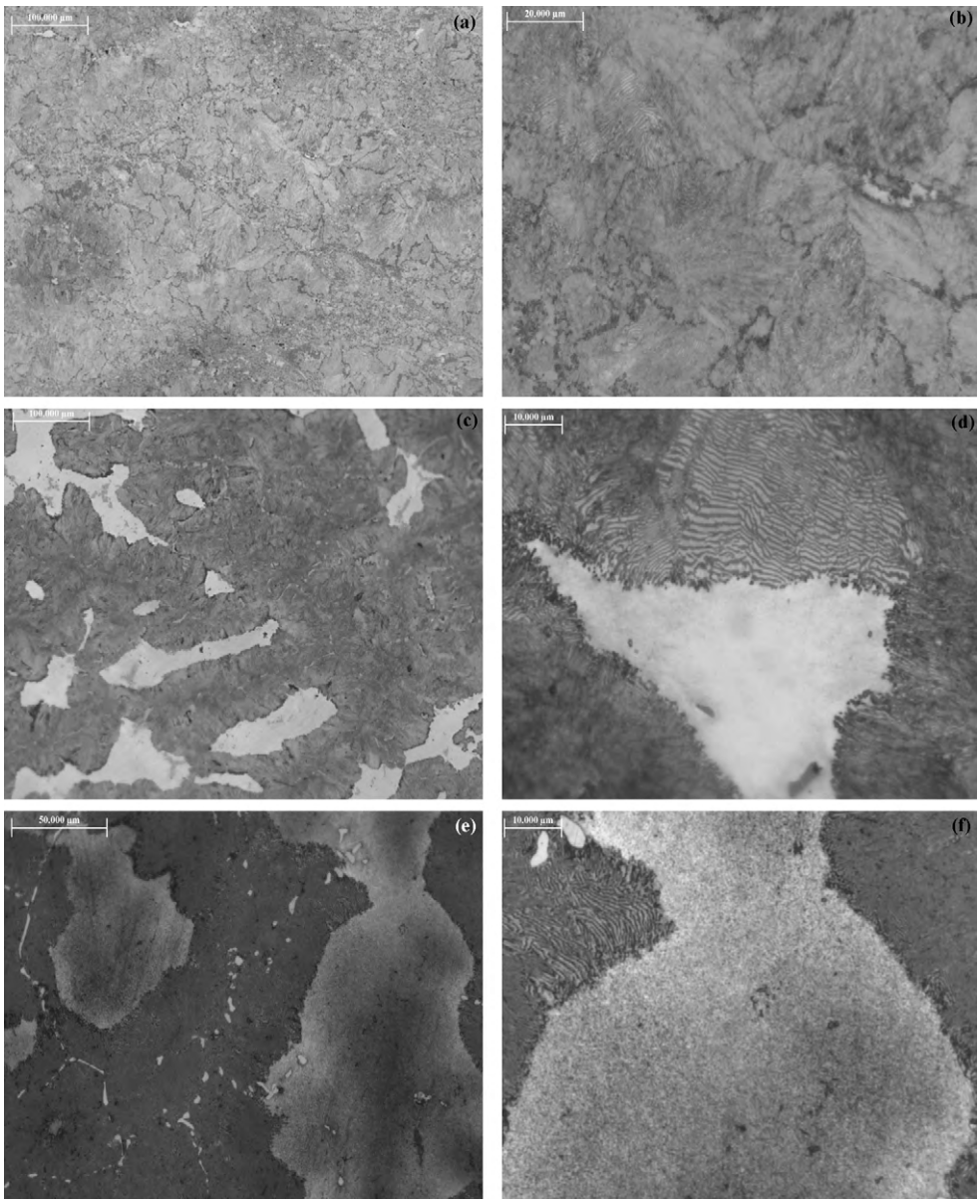

Fig. 11. Microstructure of aged U–Mo alloy at 500 °C for 68 h (a and b) U–8 wt%Mo, (c and d) U–9 wt%Mo and (e and f) U–10 wt%Mo.

3.3. *Microstructural analysis*

The microstructure of hot rolled U–8 wt%Mo alloy (see Fig. 10(a)), U–9 wt%Mo alloy (see Fig. 10(b)) and U–10 wt%Mo alloy (see Fig. 10(c)) shows equiaxed grains of cubic γ-uranium and no second phase is visible along the grain boundary. Presence of equiaxed grains reveals that dendritic structure was broken during hot rolling stage and the strains induced during rolling was completely removed due to recrystallization. Microstructure of aged U–8 wt%Mo alloy (see Fig. 11(a)) after 68 h of heat treatment at 500 °C shows the formation of second phase all along the prior gamma grain boundary which is more evident in Fig. 11(b). The microstructure of aged U–9 wt%Mo alloy for same 68 h of heat treatment at 500 °C shows the partial eutectoid decomposition of cubic γ-phase in the equilibrium products (see Fig. 11(c) and (d)). The bright region in the microstructure can be seen as γ-phase and the dark region (i.e. lamellar portion) as the decomposed product. Microstructure of aged U–10 wt%Mo alloy (see Fig. 11(e) and (f)) after 68 h of heat treatment at 500 °C again shows the bright region as untransformed cubic phase and the dark region as the product formed after eutectoid reaction.

The microstructure of aged U–8 wt%Mo alloy (see Fig. 12(a) and (b)), U–9 wt%Mo alloy (see Fig. 12(c) and (d)) and U–10 wt%Mo alloy (see Fig. 12(e) and (f)) after 240 h of heat treatment at 500 °C shows the extent of eutectoid reaction which has taken place in cubic γ-phase. The microstructures are the clear indication of the fact that U–8 wt%Mo alloy almost completely transforms to equilibrium products after heat treatment while U–9 wt%Mo alloy and U–10 wt%Mo alloy shows more resilience towards the decomposition of γ-phase in to equilibrium products.

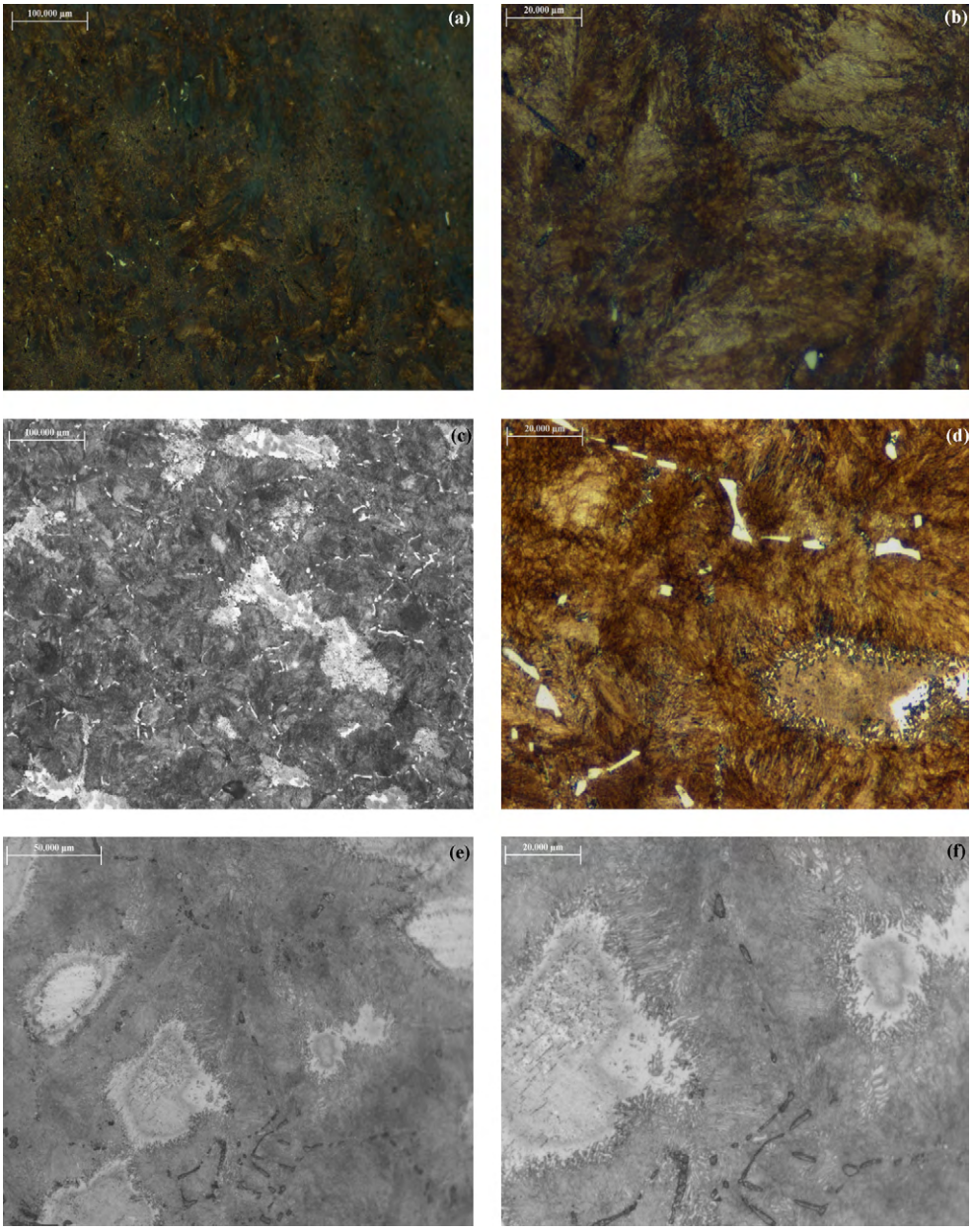

Fig. 12. Microstructure of aged U–Mo alloy at 500 °C for 240 h (a and b) U–8 wt%Mo, (c and d) U–9 wt%Mo and (e and f) U–10 wt%Mo.

4. Conclusion

From the experiments and results obtained it can be concluded that though the retention of cubic γ-phase can be done with the minimum addition of 8 wt%Mo as solute in uranium under furnace cooling condition, the cubic phase metastability is a function of molybdenum content in uranium. The extent of untransformed cubic γ-phase is more with the increase of molybdenum content in uranium which makes U–10 wt%Mo alloy more favoured one from the point of view of fuel performance during reactor operation. Another observation is the extent of eutectoid reaction in U–9 wt%Mo alloy is not as much as in case of U–8 wt%Mo alloy. Hence the choice of composition of U–Mo alloy for use as a fuel material in reactor depends on the extent one can tolerate molybdenum in uranium due to its higher parasitic neutron capture cross-section. It can also be concluded from the current study that the time given for the ageing treatment in U–Mo alloys finally determines the homogeneity of molybdenum in cubic γ-phase. The XRD patterns of various U–Mo alloys in Fig. 8 shows the broadening of γ-phase peak which means, the cubic phase is very inhomogeneous with respect to molybdenum. The XRD patterns of U–Mo alloys in Fig. 9 shows that the γ-phase peaks are relatively sharper indicating 240 h of ageing led to more homogeneity of Mo in cubic γ-phase. It can also be observed from the present study that no broadening of XRD peaks has taken place in case of α-phase during different soaking times for U–Mo alloys. This is very much expected because the maximum solid solubility of molybdenum in α-phase uranium is very low (i.e. around 1 at% at room temperature under equilibrium conditions).

Acknowledgements

The authors are grateful to Messrs. Amit Sharma and M.I. Shaikh of Atomic Fuels Division, BARC for machining uranium metal pieces in the required dimension. The authors also express their sense of gratitude to Mr. R.P. Singh, Associate Director, Nuclear Fuels Group,

BARC for providing necessary support during the course of the work.

References

[1] R.F. Domagla, T.C. Wiencek, H.R. Tresh, Nucl. Technol. 62 (1983) 353.
[2] C.L. Trybus, T.C. Wiencek, M.K. Meyer, D.L. McGann, C.R. Clark, Proceedings of the 20th International Meeting on Reduced Enrichment for Research and Test Reactors, Argonne National Laboratory Report, ANL/TD/TM99-06, 1999, p. 19.
[3] M.K. Meyer, C.L. Trybus, G.L. Hofman, S.M. Frank, T.C. Wiencek, Proceedings of the 1997 International Meeting on Reduced Enrichment for Research and Test Reactors, Argonne National Laboratory Report, ANL/TD/TM99-06, 1999, p. 81.
[4] M.K. Meyer, G.L. Hofman, S.L. Hayes, C.R. Clark, T.C. Wiencek, J.L. Snelgrove, R.V. Strain, K.H. Kim, J. Nucl. Mater. 304 (2002) 221.
[5] J.P. Durand, Y. Lavastre, M. Grasse, Proceedings of the 20th International Meeting on Reduced Enrichment for Research and Test Reactors, Argonne National Laboratory Report, ANL/TD/TM99-06, 1999, p. 28.
[6] H.B. Peacock, Coextrusion of 60 to 30 wt% U3O8 Nuclear Fuel Elements, DPST-80-447, E.I. du Pont de Nemours and Company, 1980.
[7] G.L. Copeland, Performance of Low Enrichment U_3Si_2–Aluminium Dispersion Fuel Elements in the Oak Ridge Research Reactors, Argonne National Laboratory Report, ANL/RERTR/TM-10, 1987.
[8] K.H. Kim, D.B. Lee, C.K. Kim, G.E. Hofman, K.W. Paik, J. Nucl. Mater. 245 (1997) 179.
[9] V.P. Sinha, G.J. Prasad, P.V. Hegde, R. Keswani, C.B. Basak, S. Pal, G.P. Mishra, J. Alloys Compd. 473 (2009) 238.
[10] C.-K. Rhee, S.-I. Pyun, I.-H. Kuk, J. Nucl. Mater. 184 (1991) 161.
[11] M.K. Meyer, T.C. Wiencek, S.L. Hayes, G.L. Hofman, J. Nucl. Mater. 278 (2000) 358.
[12] B.-S. Seong, C.-H. Lee, J.-S. Lee, H.-S. Shim, J.-H. Lee, K.H. Kim, C.K. Kim, V. Em, J. Nucl. Mater. 277 (2000) 274.
[13] A.N. Holden, Physical Metallurgy of Uranium, Addison-Wesley Publishing Co., Inc., USA, 1958.
[14] G. Ostberg, M. Moller, B.S. Chonning-Christiansson, J. Nucl. Mater. 10 (4) (1963) 329.
[15] D.D. Keiser Jr., A.B. Robinson, J.-F. Jue, P. Medvedev, D.M. Wachs, M. Ross Finlay, J. Nucl. Mater. 393 (2009) 311.
[16] G.L. Hofman, M.K. Meyer, Proceedings of the RERTR Conference, Sao Paulo, Brazil, October 18–23, 1998.
[17] V.P. Sinha, P.V. Hegde, G.J. Prasad, H.S. Kamath, Proceedings of the 17th Plansee Seminar, vol. 1, Reutte, Austria, 2009, RM 78/1-16.
[18] J. Lehmann, Comptes Rend. Acad. Sci. (Paris) 248 (1959) 2098.
[19] K. Tangri, G.I. Williams, J. Nucl. Mater. 4 (1961) 226.
[20] K. Tangri, D.K. Chawdhuri, C.N. Rao, J. Nucl. Mater. 15 (4) (1965) 288.
[21] H.M. Volz, R.E. Hackenberg, A.M. Kelly, W.L. Hults, A.C. Lawson, R.D. Field, D.F. Teter, D.J. Thoma, J. Alloys Compd. 444–445 (2007) 217.
[22] H. Vacelet, P. Sacristan, A. Langwille, Y. Lavastre, M. Grasse, Proceedings of the 22nd RERTR, Budapest, 1999, p. 47.
[23] V.P. Sinha, G.P. Mishra, S. Pal, K.B. Khan, P.V. Hegde, G.J. Prasad, J. Nucl. Mater. 383 (2008) 196.
[24] V.P. Sinha, P.V. Hegde, G.J. Prasad, G.P. Mishra, S. Pal, Trans. Indian Inst. Met. 61 (2) (2008) 1–6.
[25] B.D. Cullity, Elements of X-ray Diffraction, Addison-Wesley Publishing Co., Inc., USA, 1989, pp. 360–363.